Proceedings of the Korean Nuclear Society Autumn Meeting
Taejon, Korea, Oct. 2000

An Estimation of Fatigue Crack Growth in Pipe under Cyclic Four Point Bending Loads

Youn Won Park, Jin Ho Lee, Jong In Lee, and Hae Dong Chung

Korea Institute of Nuclear Safety
19 Kusung-dong, Yusung-gu, Taejon 305-600, Korea

Abstract

Fatigue crack growth estimation is very important for the assessment of piping integrity in nuclear power plants. However, the low cycle fatigue crack behavior is not yet fully understood, specially when a cracked pipe section is subjected to cyclic high bending load. In order to improve the understanding of fatigue crack growth in pipe and to compare the associated methodologies, a benchmark was proposed on the configuration of a pipe subjected to a cyclic bending. The proposed benchmark is supported by a test, performed by CEA saclay, in which a cyclic four point bending load is imposed to a pipe containing an axisymmetric notch. In this benchmark, the estimation of three stages in fracture mechanical aspects were proposed: initiation, propagation, and penetration. This paper deals with the second and the third step and the objective is to provide an appropriate procedure applicable to the estimation of fatigue crack growth in pipe for cyclic high loading case.

1. Introduction

In order to improve the understanding of fatigue crack growth in pipe and to compare the associated methodologies, a benchmark was proposed on the configuration of a pipe subjected to a cyclic bending. The proposed benchmark is supported by a test, performed by CEA saclay [1], in which a cyclic four point bending load is imposed to a pipe containing an axisymmetric notch. In this benchmark, the fracture mechanical estimation were proposed in three independent phases as follows:

- Fatigue crack initiation from a geometrical singularity
- Crack propagation under cyclic load
- Crack penetration through the pipe wall

On these three topics, many questions are not yet solved even though it is very important to

the evaluation of piping integrity and LBB application. The results on the first topic, fatigue crack initiation, was already presented [2] so that the second and the third topics will be covered in this paper.

This benchmark was proposed by CEA, and discussed by OECD/NEA PWG-3 and PWG-3 members were recommended to participate in this round robin study. In this paper the crack growth under cyclic high loading were estimated. Crack growth estimations were performed using Paris law based on the finite element analysis results, and the analytical estimation were compared with the measured defect evolution.

2. EXPERIMENTAL BASIS

The experimental basis proposed for this benchmark is the case of a pipe section submitted to a cyclic four point bending at room temperature. The pipe has an axisymetrical inside notch as a geometrical singularity, machined in the mid section of the pipe.

During the test, two different aspects were studied. The first aspect which was analyzed was the conditions of fatigue crack initiation at the singularity. Thus, the cyclic load is applied until the crack initiation detected by the Electric Drop Potential. Then, the second aspect is the crack growth under a high load amplitude from the initial defect to the total penetration through the thickness.

To determine the crack penetration, a small internal pressure is applied so that, when the defect penetrates, the fall of pressure is detected and then the test stopped. Two main data are then available: the number of cycles to cross the thickness of the pipe and the shape of the through-wall defect.

2.1 Specimen and Loading

The description of the test geometry is given on Fig. 1. In the cross section, an axisymetrical notch is machined on a depth of 1.2mm. The notch geometry is given in Fig. 1. The test was carried out under an imposed cyclic loading. Two different levels and R ratios ($R = F_{min}/F_{max}$ where F is the total load imposed by the jack) were adopted (Fig. 1):

- For the crack initiation analysis, $R = 0$
- For the crack growth analysis, $R = -1$

The material employed for this study was austenitic stainless steel 316L pipe. Material properties given for the analysis are mean characteristics of the appendix A3.3S of the RCC-MR [3] and laboratory data.

2.2 Material Properties associated with fatigue crack growth

Tensile characteristics were determined by tests on 6mm diameter specimen and can be compared to the mean values given in the appendix A3.3S [2] at room temperature: Young modulus, E = 187800MPa (192000 in [2]); Poission's ratio, ν = 0.3; Yield stress, σ_y =

235MPa (235 in [2]); Ultimate stress, σ_u = 530MPa (592 in [2]).

The mean fatigue curve of the material is deduced from the design curve given by the appendix A3.3S taking into account the safety factors 2 on the strain range and 20 on the number of cycles. Fig. 2 gives a description of the obtained best-fit curve. The Paris law given for the analysis is obtained from the laboratory data base on 316 stainless steel:

$$\frac{da}{dN} = C \cdot \Delta K^n \tag{1}$$

where C = 1.2x10^{-8}, n = 2.84, K is in $MPa\sqrt{m}$, and da/dN is in mm/cycle.

This law was obtained on CT specimen (19mm width) with a loading factor R = 0.1. The K threshold associated to this law is, K_{th}=15 $MPa\sqrt{m}$. The given crack tearing resistance also come from the laboratory data base. The normalized $J_{0.2}$ value is 490kJ/m^2.

3. Estimation of Fatigue Crack Growth

Since the initial crack length was not given in this round-robin problem, we determined it by introducing some assumptions. Then, we estimated the crack growth behavior in a pipe submitted to a cyclic four point bending.

3.1 Determination of Initial Crack Length

To determine the initial crack size and shape, it is assumed that before a crack growth, the initial crack has the shape of a full circumferential part-through crack with a = 1.2mm and no crack growth takes place in the part where K is smaller than K_{th}. Therefore the initial crack length can be considered as a part where K is larger than K_{th}. Eq. (2) was used to calculate the stress intensity factor of a full circumferential part-through crack [2] and a constant depth part-through crack.

$$K_I = \sigma_b F_b \sqrt{\pi a} \tag{2}$$

where

$$\sigma_b = M / \pi R^2 t$$

$$F_b = 1.1 + x \cdot [-0.09967 + 5.0057(x \cdot \frac{\theta}{\pi})^{0.565} - 2.8329(x \cdot \frac{\theta}{\pi})$$

$$x = a / t$$

$$\theta = c / R_i$$

$$\theta / \pi = \begin{cases} \theta / \pi & \text{for } 0 \le \theta / \pi \le 0.5 \\ 0.5 & \text{for } 0.5 \le \theta / \pi \le 1.0 \end{cases}$$

M is the bending moment. R, R_i, and t are the pipe mean radius, inner radius, and wall thickness, respectively. θ is the flaw half-angle. The a and $2c$ are the flaw depth and flaw length measured at the pipe inside surface, respectively.

We calculated K values by changing the applied bending moment and compared each K value with K_{th}. K value was equal to K_{th} when M = 24324N · m and the resultant remote stress is equal to 191MPa. Then, the location, y, was determined where the far field stress attained to 191MPa under the applied bending moment of 53000N · m and the initial crack length was determined.

$$\sin(90-\theta)=\frac{y}{R}=\frac{36.6}{79.55}$$

Consequently, θ = 62.5° and the initial crack length, $2R_i\theta$=167mm. As a crack shape, a constant depth part-through crack (CDPTC) was assumed and shown in Fig. 3.

3.2 Fatigue crack growth behavior

When the bending moment of M_{max} = 53000N · m and M_{min} = -51200N · m is applied, the plastic yield occurs even in uncracked sections of the pipe. Therefore, a correction that can consider the yielding effects of a remote stress-strain fields is necessary to evaluate the crack growth behavior using LEFM (Linear Elastic Fracture Mechanics) parameter, K.

The stress distribution occurring along the ligament of θ = 0° was corrected by using the cyclic stress-strain curve as shown in Fig. 4. According to this correction procedure, the stress values of 399MPa and 433MPa are replaced with 1699MPa and 2074MPa, respectively.

The stress intensity factor can be calculated on the constant part-through crack shape. However, it is different from the real case, which is much similar to semi-elliptical shape. To investigate the effect in K coming from different crack shape, we compared K values between a semi-elliptic part-through crack (SEPTC) and a constant depth part-through crack (CDPTC). The K equation of EPRI Report NP-6301-D was used as a K solution of SEPTC with the geometry of Fig. 4 [2]. For the pipe geometry given in this problem, the K ratios between SEPTC and CDPTC as a function of a/c is shown in Fig. 6. It indicates that the K ratio approaches the unit value of 1 according as a/c decreases. This means that the effect of the shape between SEPTC and CDPTC on the K value is negligible when the crack aspect ratio is very small like this case. Based on this observation, all K values are calculated using CDPTC formula in this analysis.

The following Paris's law is used to evaluate the crack growth behavior for each case.

$$da/dN = C(\Delta K)^m = C(K_{max}-K_{min})^m \tag{3}$$

where C = 1.2x10^{-8}, m = 2.84, K is in $MPa\sqrt{m}$ and da/dN is in mm/cycle. This law was obtained on CT specimen with a stress reatio of R = 0.1.

The effects of stress ratios on the crack growth behavior should be considered because the stress ratio of the bending moment applied to the pipe is different from that of the CT specimen. However, it is very difficult to take the R ration into account so that by letting K_{min} be 0 and neglecting the compression part of the applied bending moment, we assumed that the pipe under R = -0.97 showed the same crack closure behavior with that of the CT specimen under R = 0.1. We also assumed that there was no crack growth in the

circumferential direction because $\Delta K \leq \Delta K_{th}$.

Fig. 7 shows the crack growth behavior obtained using corrected stress. The estimated crack growth gives more or less conservative results comparing with the experimental ones.

4. Crack Penetration

We estimated the maximum crack depth and shape of the part-through crack before the crack penetrates the wall. We also estimated the shape of the through-wall crack just after the wall penetration.

4.1 Maximum Crack Depth

The J solution obtained from GE/EPRI approach is used to determine the maximum crack depth when the failure of the remaining ligament on the crack plane occurs. The J-integral estimation solution for circumferential crack front of the constant depth part-through flaw under bending moment is given as follows [3]:

$$J = f_b \cdot M^2/\pi R^4 t E' + \alpha\sigma_o\varepsilon_o t \cdot H_1 \cdot (\sigma_b/\sigma_o)^{n+1} \tag{4}$$

where

$$f_b = \frac{a_e}{t}\cdot\left[1.1+\frac{a_e}{t}\cdot\left\{-0.09967+5.0057\left(\frac{a_e\theta}{\pi t}\cdot\right)^{0.565}-2.8329\left(\frac{a_e\theta}{\pi t}\right)\right\}\right]^2$$

$$a_e = a\cdot[1+(F_b^2/6)\cdot\{(n\text{-}1)/(n+1)\}\cdot(\sigma_b/\sigma_o)^2/\{1+(\sigma_b/\sigma_o)^2 B_o\}]$$

$$F_b = 1.1+x\cdot\left[-0.09967+5.0057\left(x\cdot\frac{\theta}{\pi}\right)^{0.565}-2.8329\left(x\cdot\frac{\theta}{\pi}\right)\right]$$

$$\sigma_b = MR/I$$

$$I = \pi(R_o^4 - R_i^4)/4$$

$$B_o = [I/\{4R^3 t(\sin\beta - 0.5x\sin\theta)\}]^2$$

$$\beta = 0.5\pi(1\text{-}x\theta/\pi)$$

$$x = a/t, \theta = c/R_i$$

$$E' = E/(1-\nu^2) \qquad \text{for plane strain}$$

M is the applied bending moment. H_1 depends upon θ/π, a/t, n, and R/t. The $\alpha, \sigma_o, \varepsilon_o$ and n are constants in the Ramberg-Osgood stress-strain relation:

$$\varepsilon/\varepsilon_o = \sigma/\sigma_o + \alpha(\sigma/\sigma_o)^n \tag{5}$$

where σ_o and ε_o are reference stress and reference strain, respectively, and are related each other by the relation $\sigma_o/\varepsilon_o = E$. The σ_o is 0.2 percent offset yield strength. For the given 316L stainless steel, the values of α and n are 1.224 and 2.849, respectively.

Fig. 8 shows the changes of J-integral according as the crack depth increases. This figure indicates that the applied J is equal to $J_{0.2}$ (or J_{IC}) at the crack depth ratio of a/t = 74%. That is, as soon as the fatigue crack grows to the depth of 74% through-wall, we can

consider that this crack penetrates the pipe wall simultaneously with the initiation of tearing at $J = J_{IC}$. The maximum crack depth obtained from this result is 4.74mm.

4.2 Crack shape before the wall penetration

In this paper, a constant depth part-through flaw is assumed to be the shape of a growing crack so that the amount of crack growth to be the same value along the crack front. However, crack growth along the crack front could not be the same because of different K values. The crack growth at two different points, P1 and P2, along the crack front can be calculated from equation (6).

$$\frac{\Delta a_{P1}}{\Delta a_{P2}} = \frac{\int C(\Delta K_{P1})^m dN}{\int C(\Delta K_{P2})^m dN} = \frac{\int C\left\{\Delta\sigma_{P1}\sqrt{\pi a_{P1}}(F_b)_{P1}\right\}^m dN}{\int C\left\{\Delta\sigma_{P2}\sqrt{\pi a_{P2}}(F_b)_{P2}\right\}^m dN} \tag{6}$$

If we let point 1 be the location of maximum crack depth and P2 be an arbitrary point along crack front, fatigue crack growth of two points are given as follows:

$$\begin{aligned}\Delta a_{p1} &= \int C\left(\Delta K_{p1}\right)^m dN = C\left[\left(\Delta K_{p1}\right)^m_{a=a0} + \left(\Delta K_{p1}\right)^m_{a=a0+\Delta a} + ... + \left(\Delta K_{p1}\right)^m_{a=a0+N\cdot\Delta a}\right] \\ &\cong N\cdot\left(\Delta K_{p1}\right)^m_{a=a0+\frac{N}{2}\Delta a1} = N\cdot\left[\Delta\sigma_1\sqrt{\pi\left(a_0+\frac{N}{2}\Delta a_1\right)}(F_{b1})_{a=a0+\frac{N}{2}\Delta a1}\right]^m \end{aligned} \tag{7}$$

$$\Delta a_{p2} \cong N\cdot\left(\Delta K_{p2}\right)^m_{a=a0+\frac{N}{2}\Delta a2} = N\cdot\left[\Delta\sigma_2\sqrt{\pi\left(a_0+\frac{N}{2}\Delta a_2\right)}(F_{b2})_{a=a0+\frac{N}{2}\Delta a2}\right]^m \tag{8}$$

where $\Delta a_1 = \Delta a_{p1}/N,\ \Delta a_2 = \Delta a_{p2}/N$ obtained from the assumption that fatigue crack grows at a constant velocity from 1 to N cycle.

The fatigue crack growth ratio between two points, P1 and P2, can be determined by the ratio of (7) to (8). As shown in the figure 4, the difference in K values between SEPTC and CDPTC is negligible when aspect ration is far less than 0.1. Therefore, the contribution to crack growth from the difference in geometry factors, F_{b1} *and* F_{b2} of point 1 and 2, is assumed to be small in eq. (7) and (8). It can be said that the applied bending moment (or the stress developed by the bending moment) has the most important effect on K values under the condition of a small crack aspect ratio and the crack growth ratio can be determined approximately from the following equation.

$$\frac{\Delta a_{P1}}{\Delta a_{P2}} \approx \left(\frac{\Delta\sigma_{P1}}{\Delta\sigma_{P2}}\right)^m \tag{9}$$

The surface crack depicted in Fig. 9 is the crack shape before the wall penetration, which is derived using Eq. (9).

4.3 Crack shape after the wall penetration

To determine the shape of the through-wall crack just after the wall penetration, we have

to know the K or J solutions of the through-wall crack whose front is placed at an arbitrary angle with the radial direction as shown in Fig. 9. But is not available K or J solution that is applicable to this case. Thus we determined the shape of the through-wall crack according to the following procedure:

i) Firstly, we determine the length of the through-wall crack at which the applied J is equal to J_{IC} with an assumption that there is no part-through crack.
ii) An internal part through crack with a depth of 0.74t already exists due to fatigue crack growth and we assume the crack shape is CDPTC with a depth of a/t = 0.74.
iii) When the crack penetrates the wall thickness, the stable crack growth would stop somewhere between C1 and C2 of Fig 10.
iv) We assume that the full thickness pipe is divided by two co-centered pipes, P1 and P2 as shown in Fig. 10 and each pipe is subject to equivalent moment which produce the same stress at the extreme fiber.
v) The final through-wall crack length is determined by the equilibrium equation:

$$J_c = \frac{J_{P1(c1)} + J_{p2(c2)}}{2} \tag{10}$$

The J-integral for the circumferential through-wall crack under bending moment is estimated using Eq. (9) [4]:

$$J = f_b \cdot M^2/R^3t^2E + \alpha\sigma_o\varepsilon_o\pi R(1-\theta/\pi)^{2\cdot} \cdot H_1 \cdot (M/M_o)^{n+1} \tag{11}$$

where

$$f_b = (\theta_e/\pi)\left[1 + A\left\{4.5967(\theta_e/\pi)^{1.5} + 2.6422(\theta_e/\pi)^{4.24}\right\}\right]^2$$
$$\theta_e = \theta \cdot [1 + (F_b^2/\beta) \cdot \{(n\text{-}1)/(n+1)\} \cdot (\sigma_b/\sigma_o)^2/\{1 + (M/M_o)^2\}]$$
$$F_b = 1 + A\left[4.5967(\theta/\pi)^{1.5} + 2.6422(\theta/\pi)^{4.24}\right]$$
$$A = [0.125(R/t) - 0.25]^{0.25} \qquad \text{for } 5 \le R/t \le 10$$
$$A = [0.4(R/t) - 3.0]^{0.25} \qquad \text{for } 5 \le R/t \le 10$$
$$\sigma_b = M/\pi R^2 t$$
$$\beta = 2 \qquad \text{for plane stress}$$
$$\beta = 6 \qquad \text{for plane strain}$$
$$M_o = 4\sigma_o R^2 t[\cos(\theta/2) - 0.5\sin\theta]$$

Linear interpolation between specified values of θ/π, n, and R/t is used to calculate a value of H_1. Fig. 11 shows the changes of J-integral according as the crack length increases. This figure indicates that the length of the through-wall crack of P1 is l = 44mm at $J = J_{IC}$. and that of P2 is l = 167mm. And no unstable crack growth takes place. The external length of the through-wall crack should have a value between l = 44mm and l = 167mm. We averaged the J values at l = 44mm in P1 and l = 167mm in P2 to derive the external length of the through-wall crack. The through-wall crack depicted in Fig. 9 is the crack shape just after the wall penetration, which is determined using the above procedure. The determined internal and

external lengths of the through-wall crack are l = 167 (2θ = 125.2°) and l = 140mm (2θ = 96°), respectively.

4.4 Comparison between experimental measurements and estimations

The crack penetrates through-wall at 68cycles experimentally measured and 49cycles estimated by this study. The final crack depth just before the crack goes through out the wall is a/t = 0.74 by estimation whereas a/t = 0.77 is obtained by experiment. The crack shape in length just before and after the crack penetrates the wall is that 2θ = 112.5° in inside and 62° in outside by experimental measurements and 2θ = 125.2° in inside and 96° in outside by estimation. This comparison shows that the estimation provides slightly more conservative results than experiment and the difference are marginal. As a result, we can conclude that the proposed approach provides very reasonable results.

5. CONCLUSIONS

A fatigue crack growth was estimated as part of the round-robin problem proposed by CEA Saclay for a cracked pipe under cyclic four point bending load. The cyclic load is relatively high so that the uncracked ligament was subject to global yielding and the elasto-plastic consideration should be taken. The results obtained from analytical estimation were compared with the experimental ones and the following conclusion could be made:

(1) Through this study, an appropriate procedure applicable to estimate a fatigue crack growth in pipe under cyclic high bending load was proposed.
(2) When a cracked pipe is under relatively high cyclic bending load and the uncracked ligament is subject to yielding, the stress converted from plastic strain in cyclic stress-strain curve could be used for the calculation of ΔK.
(3) Under bending load case in pipe, the stress intensity factor equation for constant depth crack could be used for semi-elliptical crack as long as depth to length ratio, a/c, is less than 0.1.
(4) The crack shape when initiation of tearing takes place and the crack lengths in inside and ouside just after the crack goes through out the wall could be reasonably estimated by the procedure proposed in this study. The estimation results are more or less conservative than the experimental ones but they are in relatively good agreement.

REFERENCES

1. Report of the benchmark on the fatigue propagation of a semi-elliptical crack in plate subjected to cyclic bending, NEA/CSNI/R(97)8
2. Y.W. Park et al, "Evaluation of crack initiation life in notched pipe submitted to cyclic bending load", to be published in KSME.
3. A. Zahroo, Ductile Fracture Handbook, Volume 2: Constant Depth Part-throughwall Flaw,

EPRI Report NP-6301-D, Electric Power Research Institute, Palo Alto, CA, 1989
4. A. Zahroo, Ductile Fracture Handbook, Volume 1: Circumferential Throughwall cracks, EPRI Report NP-6301-D, Electric Power Research Institute, Palo Alto, CA, 1989

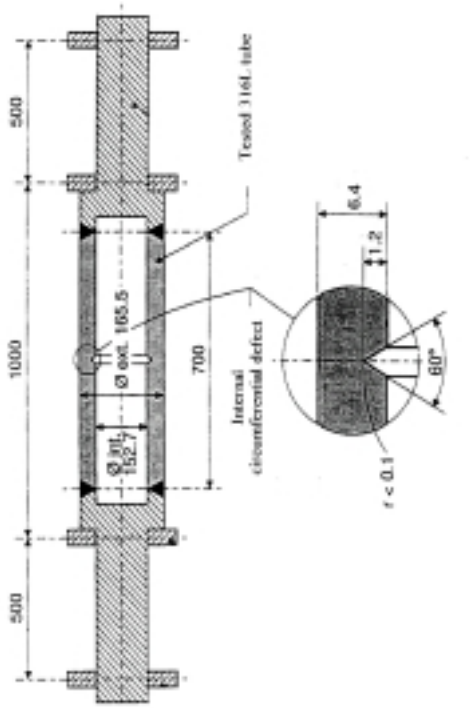

Fig. 1 Test Specimen

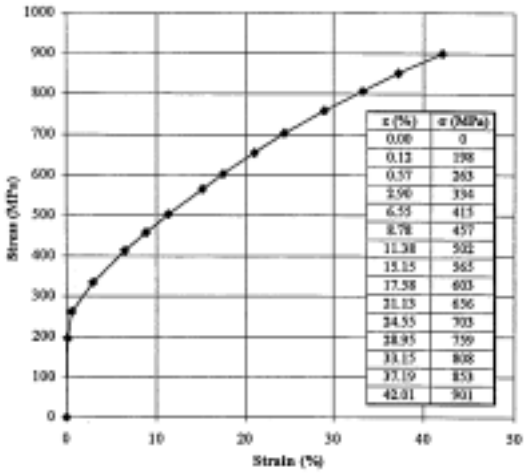

Fig. 2 Cyclic Stress-Strain Curve

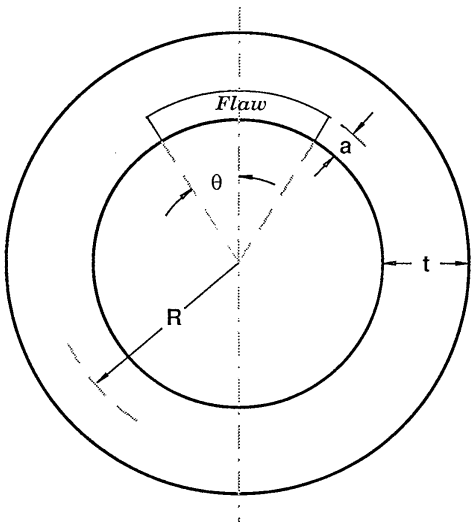

Fig. 3 Constant Depth part-through crack

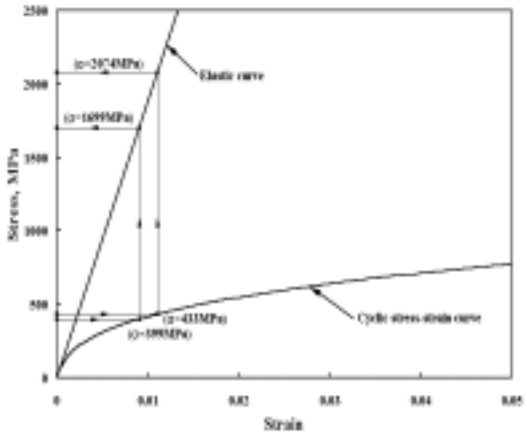

Fig. 4 Conversion of plastic strain to elastic stress

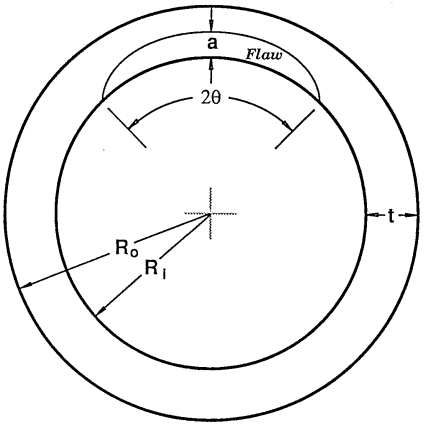

Fig. 5 Semi-elliptical part-through crack

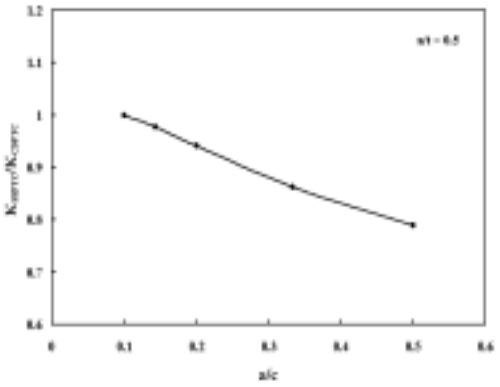

Fig. 6 Comparison of K between SEPTC and CDPTC

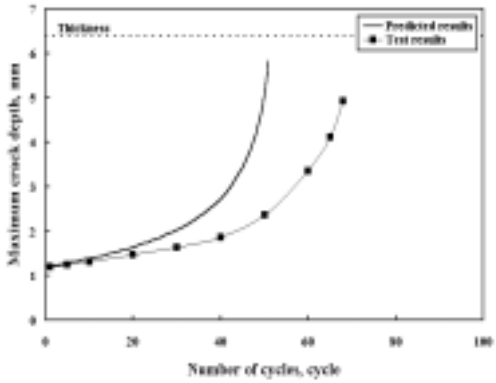

Fig. 7 Crack growth behavior using strain converted stresses

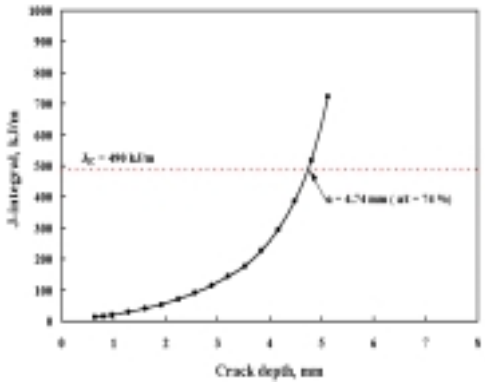

Fig. 8 J values as crack depth increases

Fig. 9 Crack shape before and after the wall penetration

Fig. 10 Cracked pipe splited by two co-centered pipes P1 and P2

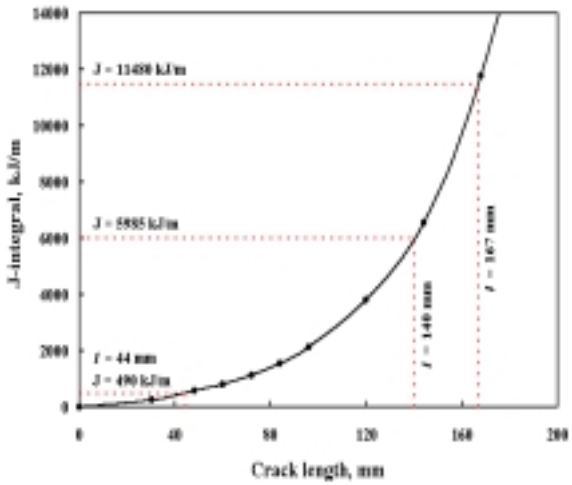

Fig. 11 J values of two co-centered pipes and determination of mean value

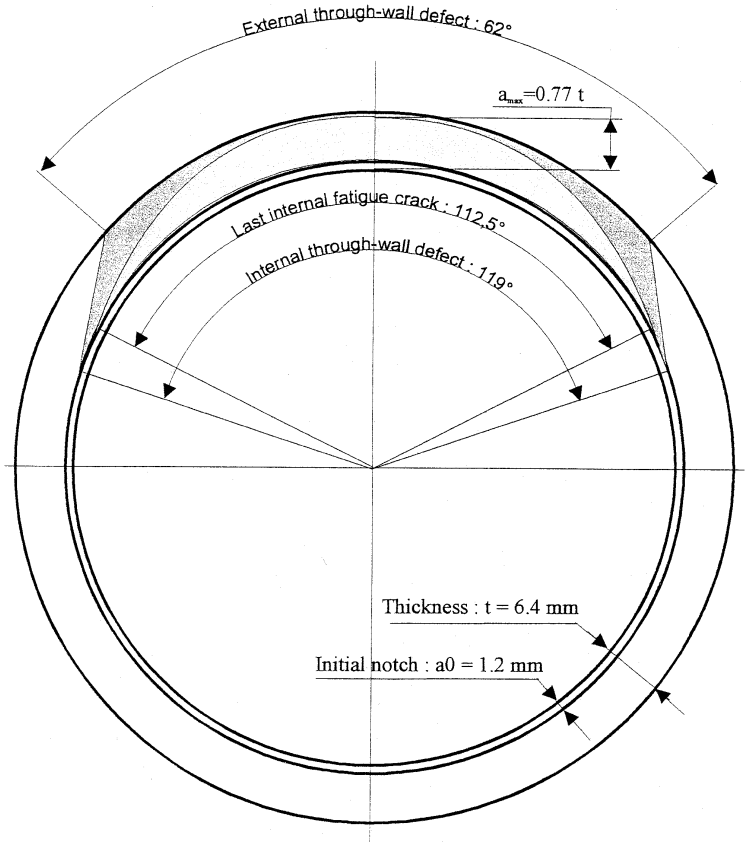

Fig. 12 Experimental measurements of crack shapes just before breaking through-wall and final through-wall